

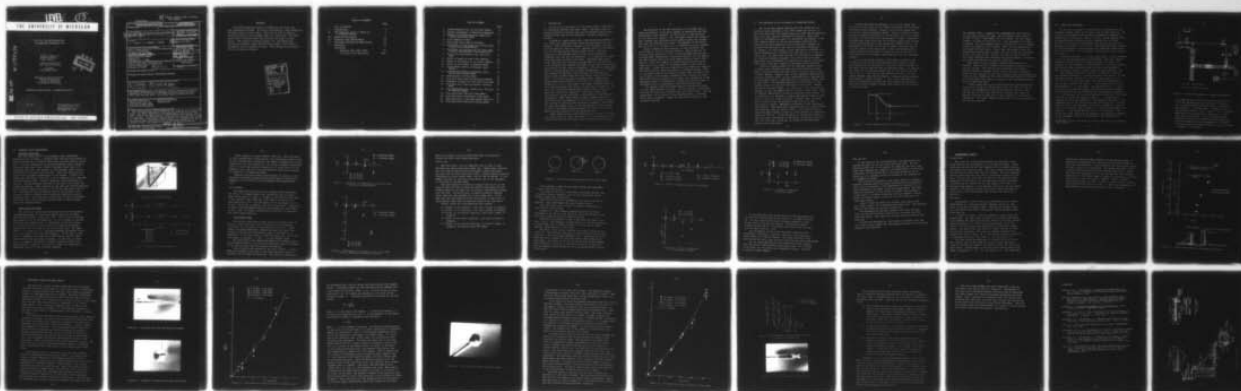
AD-A070 129 MICHIGAN UNIV ANN ARBOR DEPT OF NAVAL ARCHITECTURE --ETC F/6 20/4  
FULL SCALE WAKE AND BOUNDARY LAYER INSTRUMENTATION FEASIBILITY --ETC(U)  
MAY 79 V A PHELPS, A W TROESCH, J HACKETT N00014-76-C-1073

UNCLASSIFIED

NL

| OF |

AD  
A070129



END

DATE  
FILMED

8-79

DDC

**LEVEL**

(13)

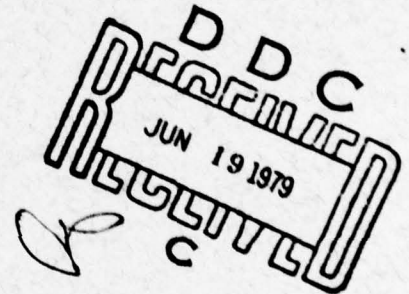
# THE UNIVERSITY OF MICHIGAN

Full Scale Wake and Boundary Layer  
Instrumentation Feasibility Study

Vernon A. Phelps, P.E.  
Research Scientist  
Project Director

Armin W. Troesch, Ph.D.  
Asst. Research Scientist

John Hackett  
Grad. Research Asst.



Department of Naval Architecture  
and Marine Engineering  
College of Engineering  
The University of Michigan

APPROVED FOR PUBLIC RELEASE: DISTRIBUTION UNLIMITED

MAY 1979

This research was carried  
out under an Office of  
Naval Research Contract  
No. N00014-76-C-1073

OFFICE OF RESEARCH ADMINISTRATION • ANN ARBOR

DDC FILE COPY

AD A070129

UNCLASSIFIED

Vernon A. /Phelps, Armin W. /Troesch  
John /Hackett

SECURITY CLASSIFICATION OF THIS PAGE (When Data Entered)

REPORT DOCUMENTATION PAGE		READ INSTRUCTIONS BEFORE COMPLETING FORM
1. REPORT NUMBER	2. GOVT ACCESSION NO.	3. RECIPIENT'S CATALOG NUMBER
4. TITLE (and Subtitle) (6) FULL SCALE WAKE AND BOUNDARY LAYER INSTRUMENTATION FEASIBILITY STUDY.		5. TYPE OF REPORT & PERIOD COVERED (9) FINAL rept.
6. PERFORMING ORG. REPORT NUMBER		
7. AUTHOR(s) V. A. PHELPS, A. W. TROESCH, J. HACKETT		8. CONTRACT OR GRANT NUMBER(s) (15) N00014-76-C-1073
9. PERFORMING ORGANIZATION NAME AND ADDRESS Dept. of Naval Architecture & Marine Engineering College of Engineering The University of Michigan Ann Arbor, Michigan 48106		10. PROGRAM ELEMENT, PROJECT, TASK AREA & WORK UNIT NUMBERS Program Element 63508N Task Area S0379001 Task 19977 Work Unit 1524-641
11. CONTROLLING OFFICE NAME AND ADDRESS Naval Sea Systems Command (NAVSEA 05R) Washington, D. C. 20362		12. REPORT DATE (11) MAY 1979
14. MONITORING AGENCY NAME & ADDRESS (if different from Controlling Office) David W. Taylor Naval Ship R&D Center Ship Performance Dept. Bethesda, Md. 20084 (12) 43 P.		13. NUMBER OF PAGES 40
15. SECURITY CLASS (of this report) UNCLASSIFIED		15a. DECLASSIFICATION/DOWNGRADING SCHEDULE
16. DISTRIBUTION STATEMENT (of this Report)  APPROVED FOR PUBLIC RELEASE: DISTRIBUTION UNLIMITED		
17. DISTRIBUTION STATEMENT (of the abstract entered in Block 20, if different from Report) (16) S0379 (17) S0379001		
18. SUPPLEMENTARY NOTES This report was prepared by the Department of Naval Architecture and Marine Engineering of the University of Michigan under contract with the David W. Taylor Naval Ship R&D Center. The contract number was N00014-76-C-1073.		
19. KEY WORDS (Continue on reverse side if necessary and identify by block number) Five Hole Pitot Tube Full Scale Wake Survey Thirteen Hole Pitot Tube Boundary Layer Scanivalve Pressure System Fluid Velocity Measurements		
20. ABSTRACT (Continue on reverse side if necessary and identify by block number) Fluid-flow measuring devices intended for full scale use were designed and tested. One device consisted of a rake supporting different types of pitot tubes. This will be used to obtain a velocity profile of the boundary layer of a test ship. The other device was a five hole pitot tube that will be used in a wake survey. The pressure transport medium (i.e. the medium that carried the pressure signal from the pitot tube to the pressure transducer) was air instead of water. This proved to be successful as the results indicate. 402 288		

# ABSTRACT

Fluid-flow measuring devices intended for full scale use were designed and tested. One device consisted of a rake supporting different types of pitot tubes. This will be used to obtain a velocity profile of the boundary layer of a test ship. The other device was a five hole pitot tube that will be used in a wake survey. The pressure transport medium (i.e. the medium that carried the pressure signal from the pitot tube to the pressure transducer) was air instead of water. This proved to be successful as the results indicate.

Accession For	
NTIS GRA&I	<input checked="checked" type="checkbox"/>
DDC TAB	<input type="checkbox"/>
Unannounced	<input type="checkbox"/>
Justification	
By _____	
Distribution/	
Availability Codes	
Dist	Avail and/or special
A	



# TABLE OF CONTENTS

	Page
List of Figures	
I. Introduction	1
II. The Selection of Air or Water as a Transport Medium	3
III. Measuring Techniques	6
IV. Boundary Layer Measurements	10
V. Instrument Package for Wake Survey	24
References	34
Enclosures	
Boundary Layer Rake Plans	35
Five Hole Pitot Tube Plans	36-37



## LIST OF FIGURES

	Page
1. System Response with the Air-Blow Method	4
2. General Arrangement of Measuring Apparatus	7
3. Example of Recorded Pressure Output for a Five Hole Pitot Tube	9
4. Pitot Tubes with Rake	11
5. Total Head Pitot Tube Calibration	11
6. The Effect of Flow Angle on the Total Head Tube Velocity Measurements	13
7. The Effect of Flow Angle on the Pitot Tube Velocity Measurements (Total Head Port)	13
8. Static Port Configuration for the Pitot Tube	15
9. Effect of Speed on Static Port Reading	16
10. Effect of Flow Angle on the Static Reading	16
11. Effect of Flow Angle on Measured Speed	17
12. Interference effects of Boundary Layer Device	21
13. Interference effects of Boundary Layer Device (with faired edge)	22
14. Determination of Flow Angle	23
15. Five Hole Pitot Tube and Mounting Assembly	25
16. Placement of Holes for Five Hole Pitot Tube	25
17. Five Hole Pitot Tube Calibration (without sand)	26
18. Drag Coefficient for a Sphere as a Function of Reynolds Number	28
19. Five Hole Pitot Tube with Sand Added	28
20. Five Hole Pitot Calibration (with sand)	30
21. Relative Error in Carriage Speed Prediction	31
22. Five Hole Pitot Tube with Fairing Added	31

## I. INTRODUCTION

The design of propellers for high speed ships is done based on information obtained from model tests. The model speed is scaled according to Froude's law, but the boundary layer, which influences the flow into the propeller, follows a Reynold's scaling.

A number of recent papers have investigated the problems of full scale wake prediction when these scaling effects are considered. Yokoo (1974) did a survey of the available literature and concluded that there are still unknown factors in the prediction of the wake pattern based on model tests. Since the character of the boundary layer in front of the propeller influences the flow into the propeller, it is important to understand what scaling effects take place. Taniguchi and Fujita (1970) show that not only does the magnitude of the velocities in the boundary layer change from model to full scale but so does the direction of the velocity components. This has an appreciable effect on the propeller race as shown by Namimatsu, *et al* (1973). They compare the estimated flow patterns of a 200,000 D.W.T. tanker based on model tests with the results from a full scale test. In a recent work done by Canham (1974), comparisons between model tests and full scale tests of a Leander Class frigate (*HMS Penelope*) were made. The author concludes there is "no significant wake scale effect in this type of frigate." However, this conclusion may be drawn from the data if only the mean wake fraction is considered. There were significant differences in local velocities in the propeller race which were unexplained. When Yokoo (1974) reviewed Canham's paper, he speculated that the supposed lack of scale effect was a result of the increase in ship wake due to surface roughness. This would increase the boundary layer of the ship making it more similar to that of the model and thus decrease the differences between model and ship velocities in the propeller race.

These papers agree in that they point out a major difficulty in current propeller design procedures, i.e., accounting for the scale effects on the wake when going from model to full scale.

The objective of the work described in this paper was to design and develop a flow meter capable of determining the wake and boundary layer character in the vicinity of the propeller of full scale test vessels. The instrument package was chosen in such a manner that the system would produce stable and reliable data over the required test range. The emphasis of the design was on *reliability*, and how *easily* a component could be replaced.

After a search of the literature, it was decided to use pitot tubes to find the velocity profile. The reliability of the pitot tube relative to other flow measurement devices such as blade wheel speed meters, ultra-sonic meters, hot film meters, and laser doppler meters has been demonstrated by Yokoo (1974). However, there are a number of problems associated with pitot tubes and in this report an alternate method of using them is described. In most previous cases when pitot tubes were used for full scale testing, water was used as a transport medium. That is, the tubes carrying the pressure signals from the head of the pitot tubes to the pressure transducers were filled with water. Should air become entrapped in the lines, the calibration of the instrument would be invalidated. A method by which the water is replaced with air is described in the following sections.

The boundary layer measurement devices included two types of pitot tubes mounted on a rake. One of these was a total head tube and the other was a Prandtl-type pitot-static tube. For the measurements in the region of the propeller wake, a five-hole pitot tube is proposed. These are described in detail in the following sections.



## II. THE SELECTION OF AIR OR WATER AS A TRANSPORT MEDIUM

One of the anticipated problems with the system was the method by which pressures on the actual measuring devices i.e. the total head tube, the Prandtl-type pitot tube and the spherical head pitot tube, would be recorded for analysis. When these types of instruments are used in a laboratory environment, it has been common practice to use the fluid whose velocities and pressures are being measured as the medium that transmits the pressure from the head of the tube to a pressure transducer. For example, in a wind tunnel a pitot tube may be connected to a mercury manometer by a flexible hose that has air in it and in a towing tank the same pitot tube may be connected to a manometer or electronic pressure transducer by a hose filled with water. When these same instruments are scaled up for use on a full-scale application, some minor laboratory problems become magnified.

Since the primary purpose of the instrument package being developed was to measure the wake velocities behind an actual ship, a natural choice would have been to use salt water as the transport medium. However, most of the transducer manufacturers' catalogs carefully spell out the undesirability or impossibility of using many types of instrumentation in corrosive fluids, such as salt water. One possible approach to the solution of this problem would be to use distilled water in the lines. However, the use of any heavy fluid, i.e., water, oil, etc., has a major drawback in that air bubbles tend to collect in the lines. These air bubbles substantially reduce the accuracy of the system. In a laboratory it is possible to remove the bubbles from the lines when the lines are relatively short. However, when the equipment is used at sea, the pressure lines will be at least fifty feet in length. Namimatsu and Maraoka (1974) experienced this problem. They substituted deaerated water for potable water and found that they got better results. One difficulty with deaerated water though is that it is not possible to completely remove all the air. If the transducer is located more than fifteen feet above the surface of the water, the partial vacuum in the line will tend to draw any air missed in the deaeration process out of the water.

A method described by Takahashi, et al (1970) shows that filling the lines with air by a method called the air-blow system eliminates these problems. Briefly, the air-blow system uses air as the pressure transport medium. Before a reading is taken, a valve is opened which blows all of the water out of the system. The valve is then closed and a measurement is taken. Potential problems that might exist with the air-blow system would include a slow system response or even undesirable dynamic effects, the magnitude of the effect of the one air-water interface, and the size and length of the tubing used. Since this method showed promise from the stand point of simplicity and reliability, it was investigated for possible implementation into the instrument package.

To test the system response, the pressure transducer was connected to one of the pitot tubes and the electronic signal was displayed on an oscilloscope. The pitot tube was placed in the water and run down the tank at different speeds. In addition, the length of the tube was varied from 10 feet (3.05 m) to 146 feet (44.5 m). The type of tube used was 1/8 inch (3.17 mm) inside diameter Tygon plastic tubing. A typical record from the oscilloscope is shown in Figure 1. The record represents the pressure measurement from when the blow pressure was stopped to when the pressure reached a steady value indicating the pressure at the pitot tube.

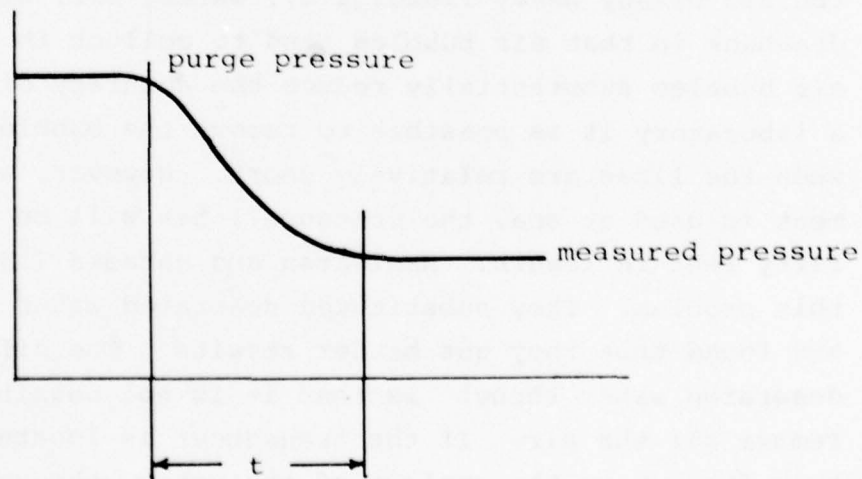


Figure 1. System Response with the Air-Blow Method

The response time,  $t$ , seemed to be independent of the velocity of the fluid at the pitot tube. For the shorter tube length of 10 feet (3.05 m),  $t$  was under 1/10 of a second. For the longer lengths of about 150 feet (45.7 m),  $t$  was estimated to be about 3 seconds. For the proposed length of 50 feet (15.24 m)  $t$  reached a value of around 6/10 of a second. There are two observations to be made from the figure. First, the time needed to have the system reach steady state is small relative to the time available in the full scale trials. Second, the lack of oscillations in the record indicates the system has sufficient damping to minimize any dynamic effects due to resonant vibrations.

The effect of the air-water interface was difficult to measure. There will be a pressure drop across the surface due to surface tension. This drop will be proportional to surface curvature and will increase as the size of the holes decreases. Since the test results for the total pressure tube, as described in a later section, compare so well with the carriage speed, the effects of the air-water inter-face, as applied to the instrument package, will be considered small.

Finally there were no noticable differences encountered when 1/16 inch (1.59 mm) ID tubing replaced the 1/8 inch (3.18 mm) ID tubing. We recommend that the larger diameter tubing be used for the part of the lines carrying the flushing air, while the smaller lines may be used for the tubes leading to the pressure transducer. For a more complete description of the test apparatus, see the next section.



### III. MEASURING TECHNIQUES

At the initial stages of this project, the decision on the transport medium, either air or water, had not been made yet. As a result, the measuring and recording systems were designed to handle both air and water. While it quickly became apparent that the deaerated water process was more complex than air-blow process, it could not be eliminated until the air-blow process was proven successful. As a result, some components were included in the first design of the measuring and recording systems which were not necessary. For a schematic representation of the device, see Figure 2.

The water reservoir D and the glass tubes K were intended for use in the deaerated-water-flush system. Once the air-blow system was proven effective, these parts were not used. The manifold N was necessary, because without it, the lines leading to the pitot tubes would have seen different blow pressures. This could have resulted in some lines not being purged at all.

The manometer was used to provide a calibration check on the pressure transducer. In this procedure, the valve at B was partially opened, allowing a pressure of approximately 3 psi ( $2.07 \text{ N/cm}^2$ ) to enter the lines. The off-on Scanivalves\* at L and M were closed. The cock at G was closed and the one to the manometer at H was opened. The Scanivalves at I and J were set on the same tube number allowing the pressure measured by the manometer to also be measured by the pressure transducer

O. The pressure acting on the manometer and pressure transducer could be varied by the regulator valve C. In this way, a calibration curve was produced for the pressure transducer. The transducer was of the differential type with two ports. One port was left open to the atmosphere giving the transducer a range of  $\pm 4$  psi ( $\pm 2.76 \text{ N/cm}^2$ ) gauge pressure. To zero the transducer, the valve at C was closed and the cock at G was opened. This vented the lines connecting the manometer and pressure transducer to the atmosphere giving the transducer a zero differential.

---

\*Scanivalve is the trade name of a device that acts as a pressure multi-plexer.



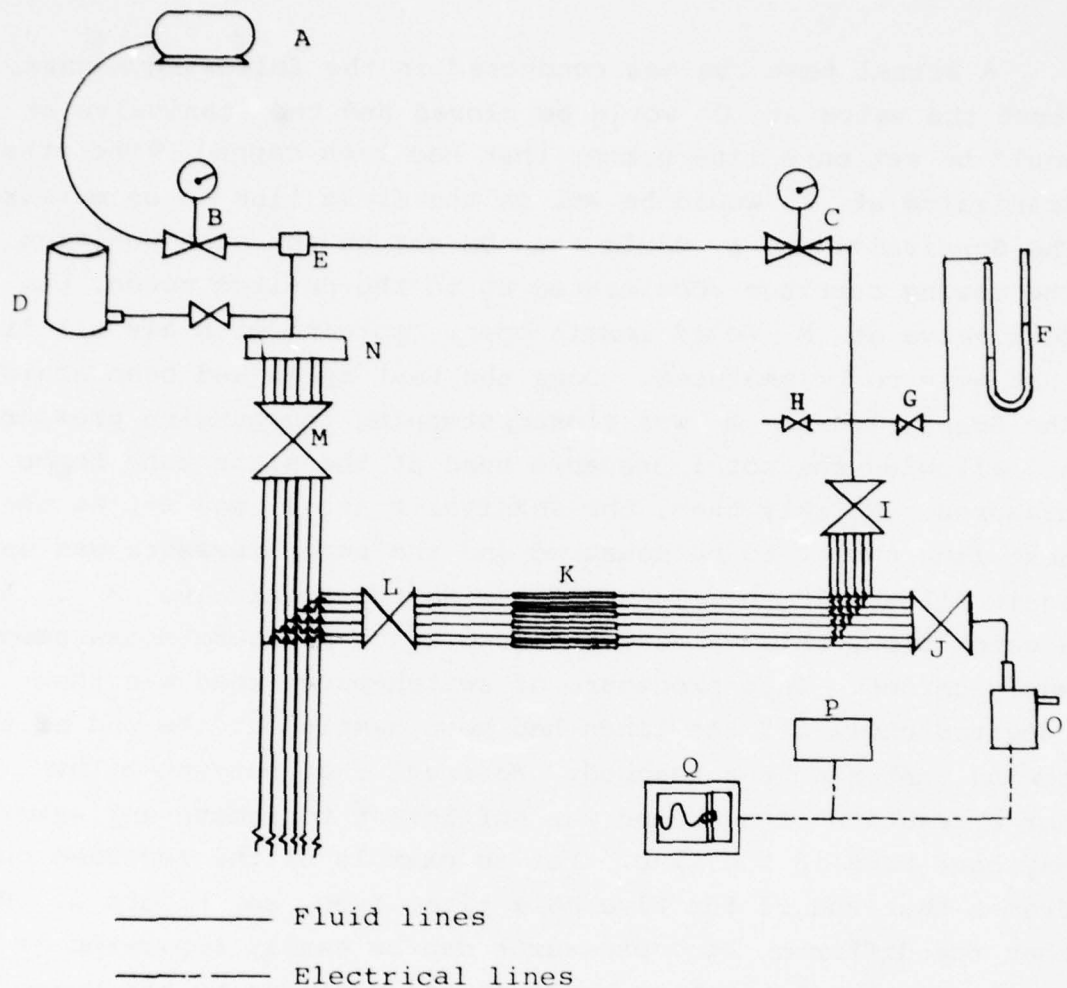
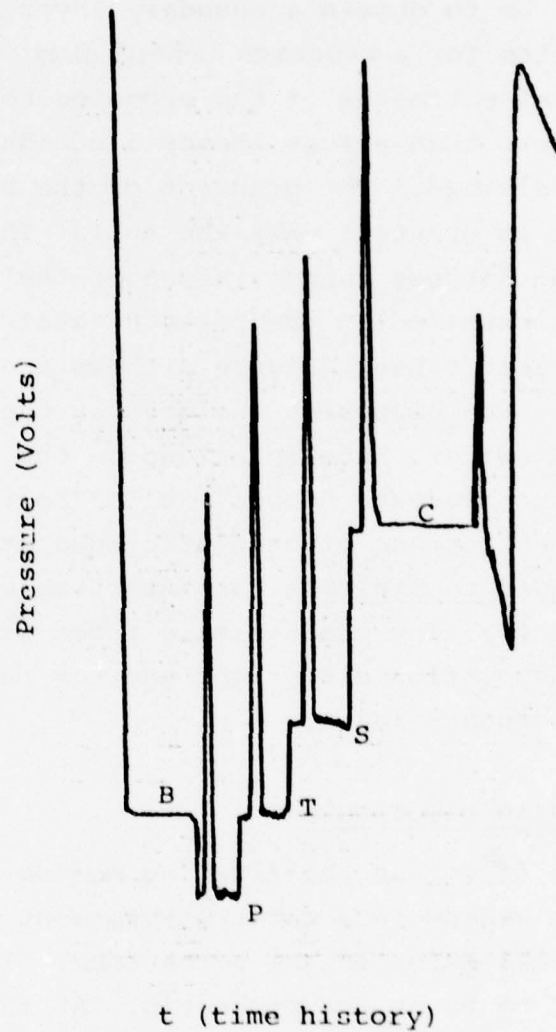


Figure 2. General Arrangement of Measuring Apparatus

A air compressor and 2.5 gal (9.46 lit) tank rated at 100 psi ( $68.9 \text{ N/cm}^2$ ) and pumping rate of 2 gal/min (7.57 lit/min); B and C regulator valves with pressure gauges; D deaerated water reservoir, E three-way valve; F manometer using 2.94 specific gravity fluid; G and H cocks; I and J Scanivalve, model W0601/1:-12T 12 input lines, 1 output line; K glass tubes 1/4-inch (6.35 mm) OD; L and M Scanivalve, model W1260/6P-1T, 6 input lines 6 output lines, (these valves acted as off-on switches for 6 lines simultaneously); N manifold; O two port, differential pressure transducer  $\pm 4 \text{ psi}$  ( $\pm 2.76 \text{ N/cm}^2$ ); P voltmeter; Q x-y plotter.

A actual test run was conducted in the following manner. First the valve at C would be closed and the Scanivalve at I would be set on a line number that had been capped. The other 12/1 Scanivalve at J would be set on the first line to be measured. The Scanivalve at L would then be set on the open position. As the towing carriage accelerated up to the desired speed, the Scanivalve at M would remain open, purging with air all lines that were to be measured. Once the test speed had been achieved, the Scanivalve at M was closed, stopping the purging pressure and allowing the total pressure head at the pitot tube to be measured. Quickly then, the Scanivalve at J was set at the next line number to be measured and the purge pressure was once again allowed in the lines by opening the Scanivalve M. After a quick blow, this valve was closed and a pressure measurement was recorded. This procedure of switch-purge-read was then repeated until all the lines had been sampled or the end of the towing tank had been reached. We found that purging a line for a fraction of a second was sufficient to remove any water that may have been in the line. For an example of the recorded output from a test run of the five hole pitot tube, see Figure 3. Note that the different line pressures can be easily separated as a result of the distinctive peaks in the plot due to the purge pressure. The chart rate was 2.5 sec/cm.

The ease with which the numerous measurements could be made was impressive. Having only one pressure transducer reduced the amount of time needed for electronic balancing and calibration. The regulator and pressure gauge at C were redundant and found not to be necessary. The Scanivalves were hand operated which resulted in some blow times that were too long and some pitot-pressure measurements that were too short. Driving these valves by an electric motor should remove this difficulty.



Symbols for 5 hole Pitot tube:

B - bottom hole

P - port hole

T - top hole

S - starboard hole

C - center hole

Figure 3. Example of Recorded Pressure Output for a Five Hole Pitot Tube.

#### IV. BOUNDARY LAYER MEASUREMENTS

##### BOUNDARY LAYER RAKE

The first application of the boundary layer measurement devices will be to obtain a boundary layer velocity distribution on the hull bottom for a research vessel along the after section of the hull. Initial estimates of the expected boundary layer thickness there were less than a foot, hence a boundary layer rake of 12 inches was selected. The gradient of the boundary layer velocity distribution is greatest near the hull. This then should be the region of the largest concentration of the probes. A total of 10 probes were installed in the rake, 8 total pressure pitot tubes and two pitot-static tubes. Figure 4 shows the rake with probes installed. See the blueprint enclosed at the end of this report for a detailed drawing. Tube locations on the rake were labeled starting with the probe nearest the hull as "A" to the outer-most probe as "J". Placement of one pitot-static tube at the outermost rake position tended to minimize the interference effects, as will be discussed later. The pitot-static tubes will be used to determine the static head, flow direction, and how each of these changed within the boundary layer.

##### TOTAL HEAD PITOT TUBE

The use of air as the flushing medium and also the pressure transmission medium in a water environment meant an air-water interface would exist in the pitot tube. This vertical interface was expected to be at the probe tip. At the interface of any two fluids one must contend with the phenomenon of surface tension. As a result of surface tension there is a pressure difference between the water side and the air side of the film. The magnitude of the surface tension (and hence pressure difference) varies in inverse proportion to the tube diameter. If the tube is very small in diameter, the effect of surface tension must be taken into consideration during data analysis. If the tube is fairly large in diameter, the effect of surface tension is small and may be ignored. With the latter goal in mind, our tubes were a reasonably large 1/4 inch (6.35 mm) diameter.



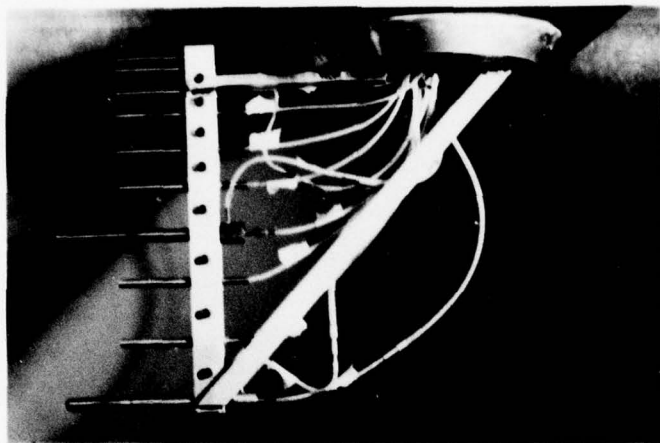


Figure 4. Pitot Tubes with Rake

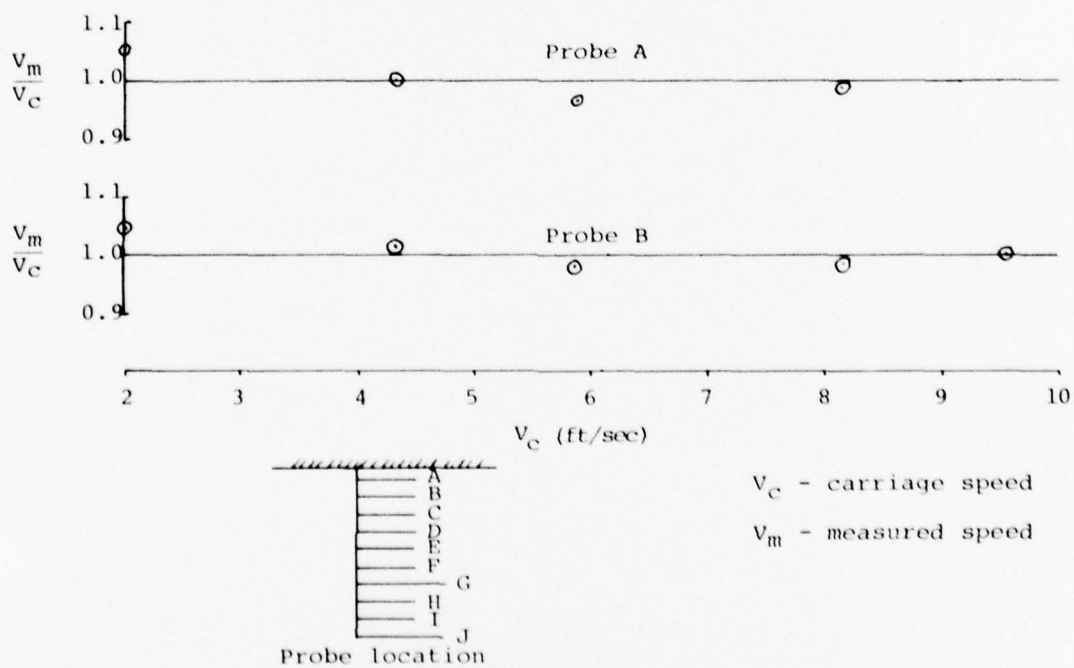


Figure 5. Total Head Pitot Tube Calibration

Other reasons for large diameter tubes are, less likelihood of tube clogging due to small marine life and marine pollution and greater strength hence minimizing the chance of damage during rake installation and test operations. Too large a diameter tube would result in an average pressure reading over a large region of the boundary layer, and large flow perturbations which may influence the readings of neighboring probes.

Therefore the probe design selected here is similar to the apparently successful Japanese design described by the Executive Committee for the Project of Ship Boundary Layer Measurements (1971).

#### *TUBE PERFORMANCE*

The tubes gave excellent static readings while motionless. The effect of forward speed after subtracting out the static head, can be seen in Figure 5. Figure 6, the effect of the angle of the incident flow, shows the total head is insensitive to flow angles up to  $10^\circ$ . At flow angles of  $20^\circ$  and speeds of 10 ft/sec (3.05 m/sec) or greater, the error is below 2%. Therefore, we expect good performance from the total head pitot tubes when at sea. This, of course, depends upon our ability to determine the static head accurately.

#### PITOT-STATIC TUBE

The classic pitot-static tubes such as the Prandtl tube are known for their ability to give flow speed directly without correction for flow angle at flow angles of up to  $15^\circ$ . These probes can supply additional information about the flow. The purpose of placing the pitot-static tubes in the rake is to determine, 1) the static head, 2) the flow direction, and 3) the flow speed, at location G and J in the boundary layer.

Our pitot-static tube design was based on the common single fluid probes design i.e. the fluid in which the probe is operating in is also the fluid used for pressure transmittal.

A pitot-static tube consists of two sets of ports - a total head port located at the nose of the probe and static port(s) located along the shaft of the probe. The design of these ports

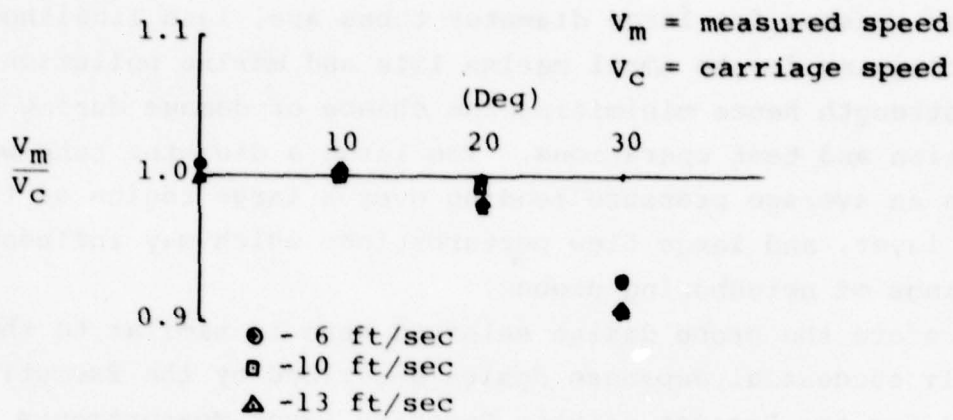


Figure 6. The Effect of Flow Angle on the Total Head Tube Velocity Measurements.

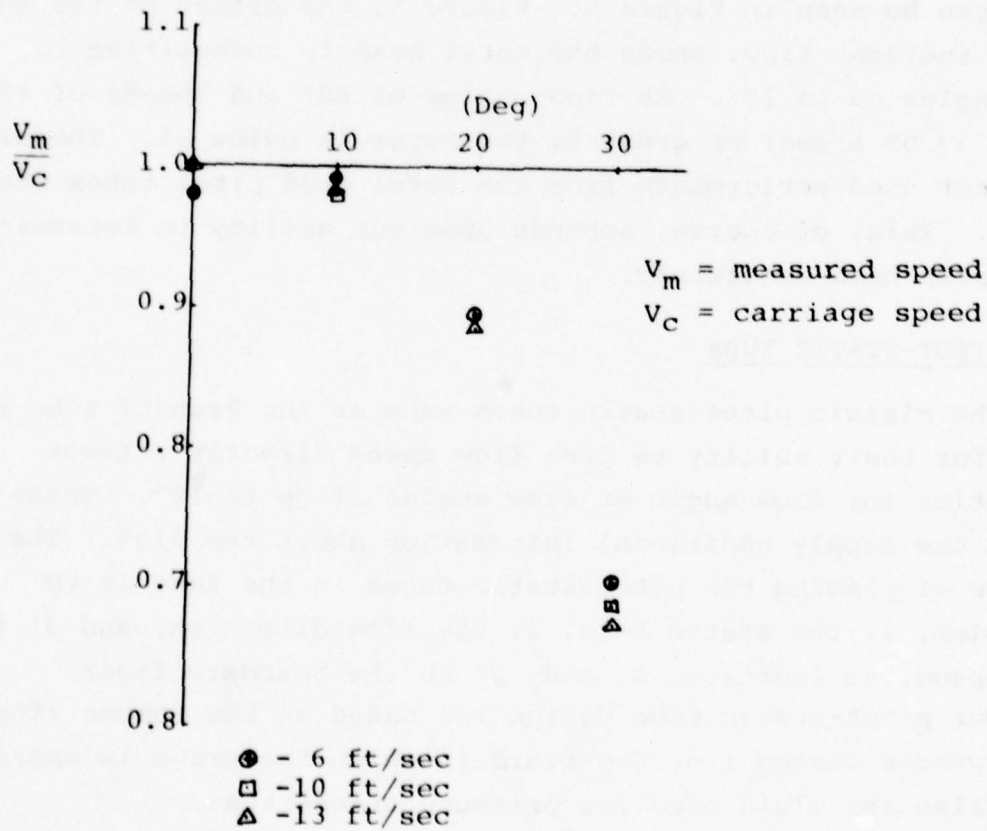


Figure 7. The Effect of Flow Angle on the Pitot Tube Velocity Measurements (Total head port)

had to be altered from the single-fluid base line design to reflect the dual fluid system used here.

#### STATIC PORT

The static-port plays an important role in that it must determine the static head while under way. These static readings will not only be used with the pitot-static tube total head, but also with the total head pitot tubes. Several design questions concerning the static ports arose, such as the following: 1) the number of ports, 2) the size of the ports, and 3) the placement of the ports on the tube shaft.

The ports should be located far enough from the tip of the probe so that the flow is along the shaft of the probe, yet far enough forward of the rake so as to minimize interference effects with the rake. The static port is usually located a distance three times the tube diameter aft of the probe nose. At the same time the tube length from the static port to rake strut is taken between eight and ten times the width of the rake strut.

Several static port configurations were tested:

- 1) 4 holes, in x-y position, 1/32 inch (.79 mm) in diameter
- 2) 4 holes, in x-y position, 1/16 inch (1.59mm) in diameter
- 3) 8 holes, in x-y and 45° position, 1/16 inch (1.59mm) in diameter
- 4) 1 hole, in the minus y position, 1/16 inch (1.59)mm in diameter
- 5) 8 holes, in x-y and 45° position, 1/16 inch (1.59mm) in diameter, with sand around tube shaft.



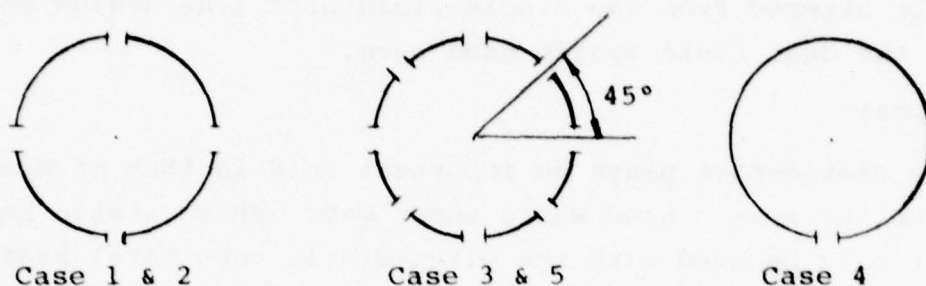


Figure 8. Static Port Configuration for the Pitot Tube

Fig. 8 shows a cross section taken through the tube shaft in way of the static port.

The probe in the first configuration performed poorly, the air-water interface appeared to be at the static port, hence surface tension was significant.

Case two had the ports enlarged to 1/16 inch (1.59 mm) in diameter. Tube performance was significantly better.

Case three was tried in order to minimize sensitivity to cross flow or vortex flows.

Because of a time response problem associated with the breakdown of the surface film and water entering the tube, a one static port tube was tried as shown in Case 4.

Open water performance of case 4 was about the same as for case 2 and 3. The response of probe types 2, 3, and 4 in position J while under way is shown in Figure 9. No one of the three designs seems superior to the other.

The effect of horizontal flow angle for case 4 can be seen in Figure 10. The vertical flow angle is zero with the tube in rake position J. Note the speed dependence here. Combining the total head and static reading for the pitot-static tube produces the flow speed. In Figure 11 one can see how this net speed changes with flow angle. An error of less than 4% exists to about 30° with no apparent speed dependence for flow speeds above 10 ft/sec (3.05 m/sec).

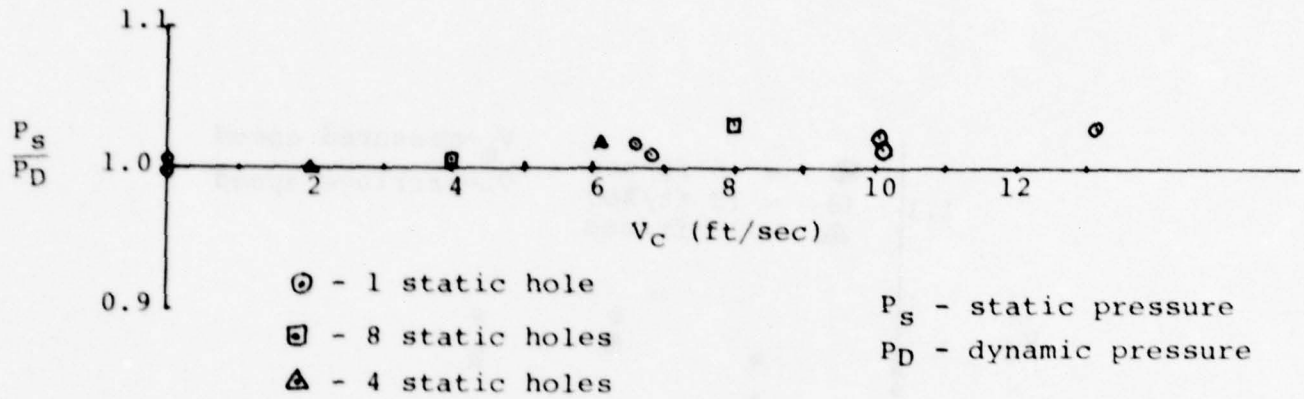


Figure 9. Effect of Speed on Static Port Reading.

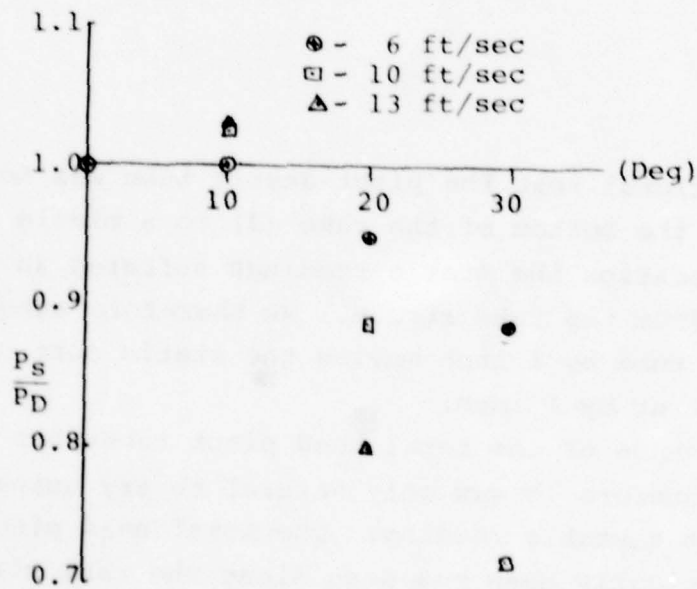


Figure 10. Effect of Flow Angle on the Static Reading

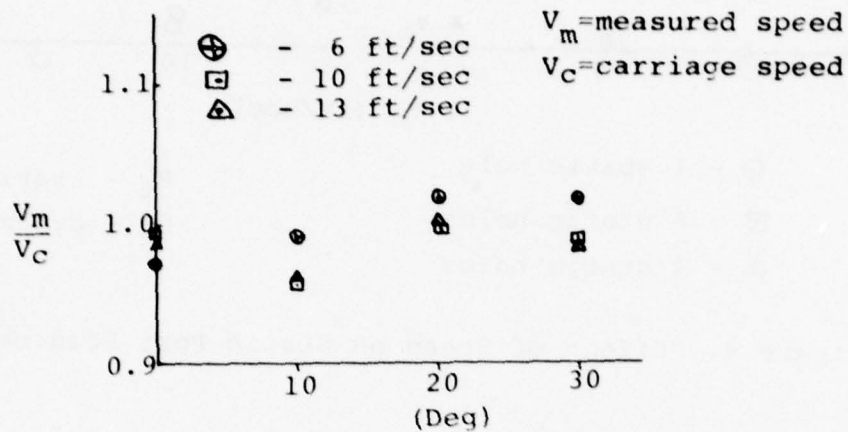


Figure 11. Effect of Flow Angle on Measured Speed

As an additional test the pitot-static tube was moved from its position at the bottom of the rake (J) to a middle position (G). At this location the static readings suffered an interference effect from the rake struts. We therefore suggest lengthening the tube by 1 inch moving the static port out away from the rake strut by 1 inch.

The performance of the total head pitot tubes has been outstanding, therefore it was only natural to try using one of these probes for a static reading. One total head pitot tube was mounted vertically open end down along the rake strut and tested.

For low speed applications this probe gave better results than the static reading from a pitot-static tube. At 13 ft/sec (3.97 m/sec) the two probes gave comparable results. We have no data at higher speeds.

#### TOTAL HEAD PORT

In the design of the total head port, the same design considerations apply as for the total head pitot tube. The two important points are 1) the results of combining the static and total head readings must produce a flow speed which is relatively insensitive to flow angles and 2) the probe should not be so large that it's presence alters its reading or the readings of its neighboring probes.

The first point requires a nose design which will produce pressure readings which will match the static ports readings in such a way as to produce a flow speed which is constant for at least 20 degrees, the range of the total head tubes. The hemispherical head such as that used on a Prandtl tube produces a larger region of constant flow speed than say Brabbee's design which has a head similar to that on our total head tube, i.e. "open tube design."

Figure 7 shows the effect of incident flow angle on the total head reading for a hemispherical design nose. The resultant speed vs flow angle can be seen in Figure 11.

The hemispherical head does produce total head readings which are more directionally sensitive to flow than the total head tube design. This fact will be used to help determine flow direction.

To make the hemispherical head probe a reasonable size and still have a large enough port the dimensions shown in the enclosed blueprint were selected.



## INTERFERENCE EFFECTS

### UNIFORM STREAM

The first set of tests were designed to determine if one probe effected the performance of its neighboring probe. These tests were carried out by first removing all the probes from the rake except for one pitot tube. The test jig was then towed down the tank and the pitot tube results recorded. This was repeated several times with the pitot tube in a different location on the rake. All the tubes were then installed in the rake and towed. Comparison of the results for the individual probe at different locations and the results for all the probes in the rake in a uniform stream showed, no interference effects on the total head readings. As reported earlier interference effects between the static port on the pitot-static tube and the rake strut were detected.

### WAKE SCREEN

The purpose of these tests was to determine how the probes would behave in a velocity gradient somewhat similar to that found in the ship's boundary layer. Because the boundary layer is a rotational flow field, interference effects between probes might show up.

In order to create a velocity gradient, a wake screen was constructed. The wake screen was made up of a wood frame 18x18 inch (460x460 mm) square with several layers of different density screens mounted on it. The first screen was made up of four layers of screen ranging from chicken wire to household window screen. The screen face was placed 12 inches (300 mm) in front of the pitot tube head. The velocity gradient produced here ranged from  $.85 V_C$ , where  $V_C$  is the uniform stream, at position J (outermost position on the rake) to  $.4V_C$  at position B.

The wake screen was modified for a second series of tests. The trailing edge of the frame was faired and two additional layers of screen were added to the upper 6 inches (152 mm) of the wake screen. This produced a velocity profile which ranged from  $.85V_C$  at position J to  $.3V_C$  at position B. The tests were

carried out using the same procedure as the uniform stream i.e. removing all probes but one, then testing that single probe at different rake positions. This allows the velocity profile behind the wake screen to be constructed. No attempt was made to model a typical turbulent boundary layer with the wake screen. Next, all tubes were installed in the rake and the test was repeated. Comparison of the results shown in Figure 12 and Figure 13 indicate that there are some interference effects. Figure 12 shows interference effects at tube J and B , while Figure 13 shows a strong interference effect on tube F . This was probably due to the presence of the large pitot-static tube in position G .

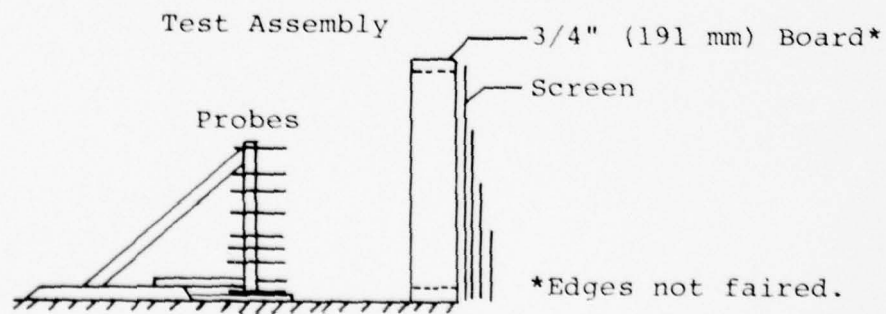
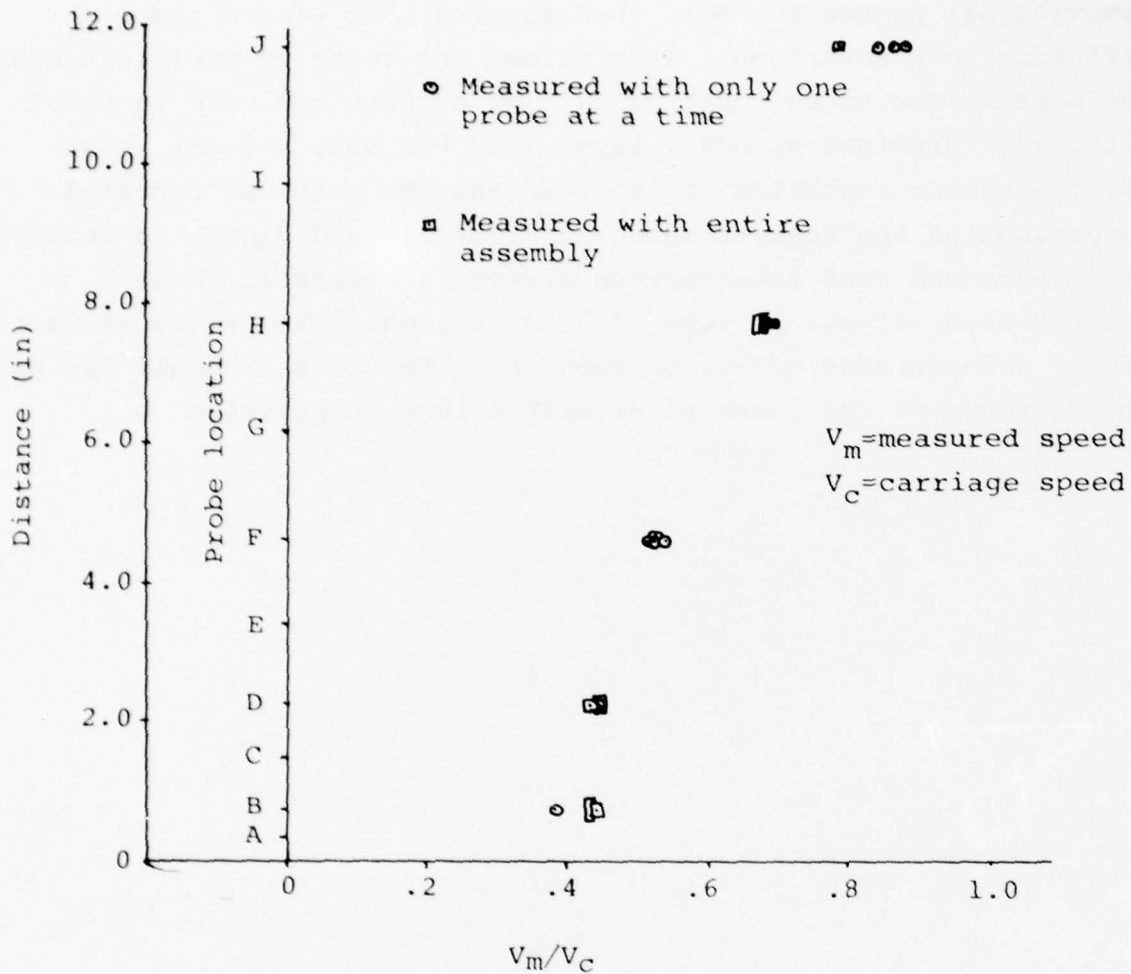
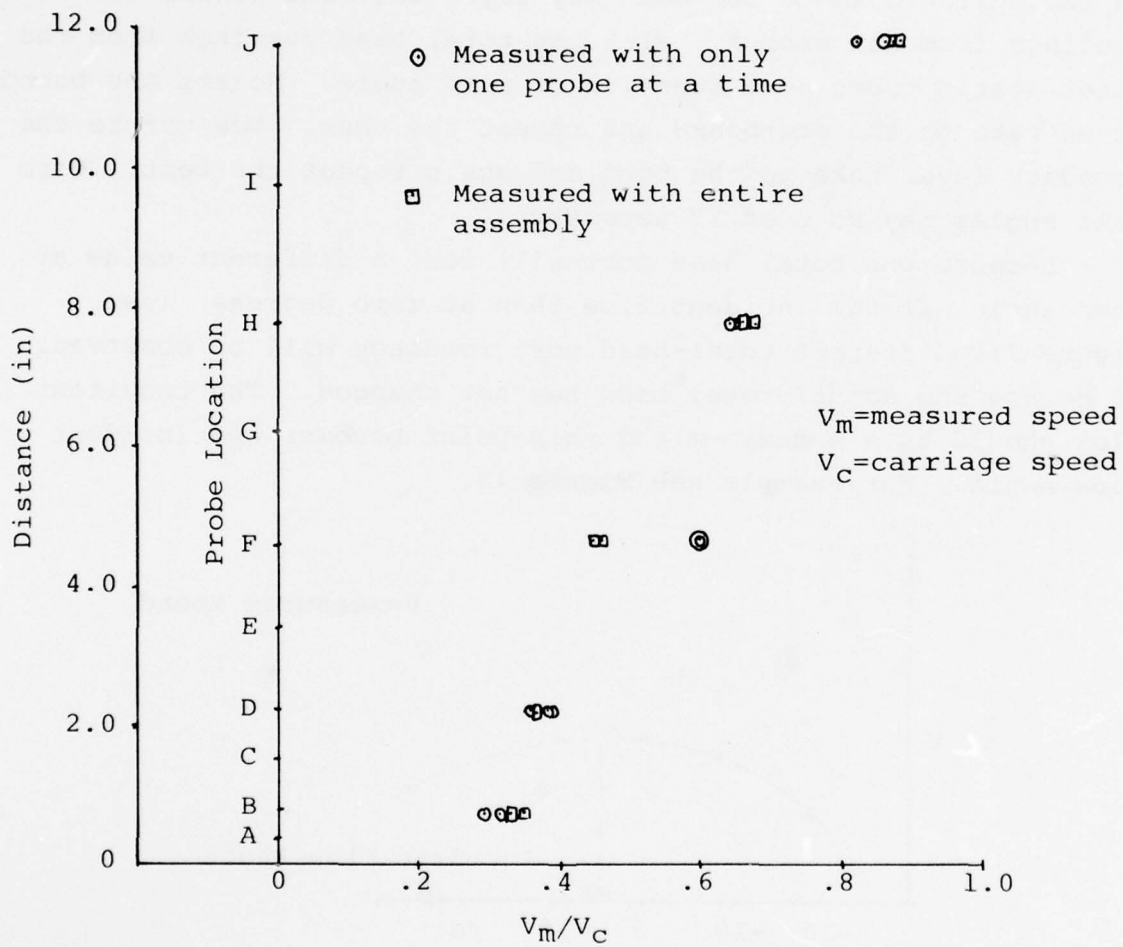


Figure 12. Interference effects of Boundary Layer Device



Test Assembly: Same as shown in Figure 12 except for the following:

- 1) Edges of 3/4" (191 mm) board faired
- 2) More screen was added; two pieces extending 6" (152 mm).

Figure 13. Interference effects of Boundary Layer Device (with faired edge)



#### DETERMINATION OF FLOW ANGLE

The incident fluid flow angle can be determined by taking advantage of the sensitivity of the total head port of the pitot-static tube to the flow angle. Assume an incident flow angle exists when the boundary layer rake is mounted in its zero position on the hull. Conduct the boundary layer test and record the readings from all probes. Plot the total head readings from the pitot static tubes as a function of rake angle. Rotate the boundary layer rake to the starboard and repeat the test. Now rotate the boundary layer rake to the port and again repeat the test. More rake angles may be used if necessary.

Because the total head port will read a different value at some angle off the incident flow than at zero degrees (see Figure 7), different total-head port readings will be observed. Of course the actual total head has not changed. The resultant plot should have a maximum and this point becomes the incident flow angle. For example see Figure 14.

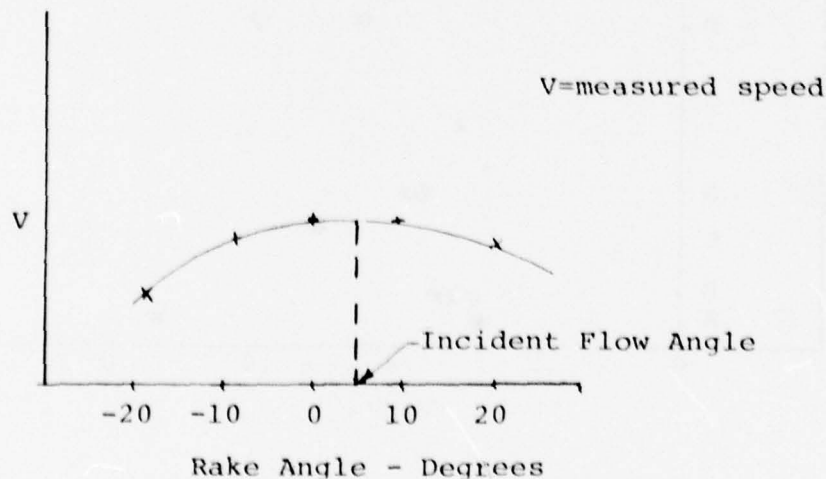


Figure 14

One of these plots will be produced for each pitot-static tube. If another pitot-static tube in the same rake produces a plot which yields a different incident flow angle it would imply that the flow direction is changing through the boundary layer, a phenomenon not unheard of in a rotational flow.

## V. INSTRUMENT PACKAGE FOR WAKE SURVEY

The main goal of this research effort was to get reliable velocity profiles in the wake of a full scale ship. As described earlier, it was decided to use five hole pitot tubes in a manner similar to that described by Pien (1958). The major difference between our equipment and Pien's (1958) was that the full scale measurements were to be taken with air instead of water in the lines. This has been used successfully by Takahashi et al (1970), among others. For a detailed drawing of the five hole pitot tube and its mounting assembly, see the blueprint enclosed at the end of this report. A photograph of the instrument is shown in Figure 15.

The location of the holes on the 2-3/8 inch (60.3 mm) spherical head was as follows: one hole to be placed on the centerline and the other four holes to be placed at an angle of 30° (port and starboard, top and bottom) from the centerline. Figure 16 shows the placement of the holes. One anticipated benefit from this particular hole placement was that the pressure differences between outside holes and the center hole would be larger and thus less susceptible to scatter than the pressure differences for a hole placement that had the outside holes nearer to the centerline. While in principle this reasoning may be correct, the fact that the fluid was viscous presented a number of problems. These problems and the steps taken to solve them are described below.

An attempt was made to calibrate the pitot tube assembly using the procedure outlined by Pien (1958). Pien states that within a region enclosed by a 40° angular distance from the stagnation point, the pattern of pressure distribution is "nearly independent of Reynold's number." Unfortunately, our results indicated that for the range of pitot tube sizes being tested, a definite Reynold's number effect was present. This can be seen from Figure 17 where the non-dimensional pressure coefficient  $(-CS+CP)/(CS+CP)$  is plotted vs.  $X$ , the angle in the horizontal plane between the incident flow and the centerline. Here  $CS$  and  $CP$  represent the pressure differences between the center hole and

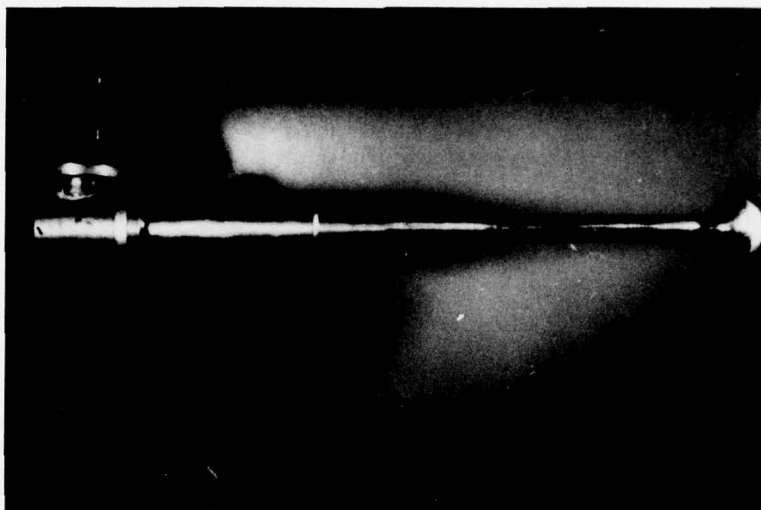


Figure 15. Five Hole Pitot Tube and Mounting Assembly

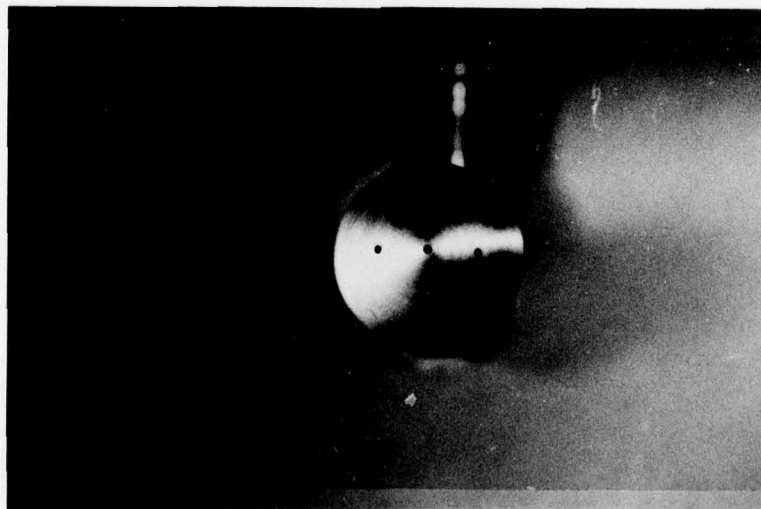


Figure 16. Placement of Holes for Five Hole Pitot Tube

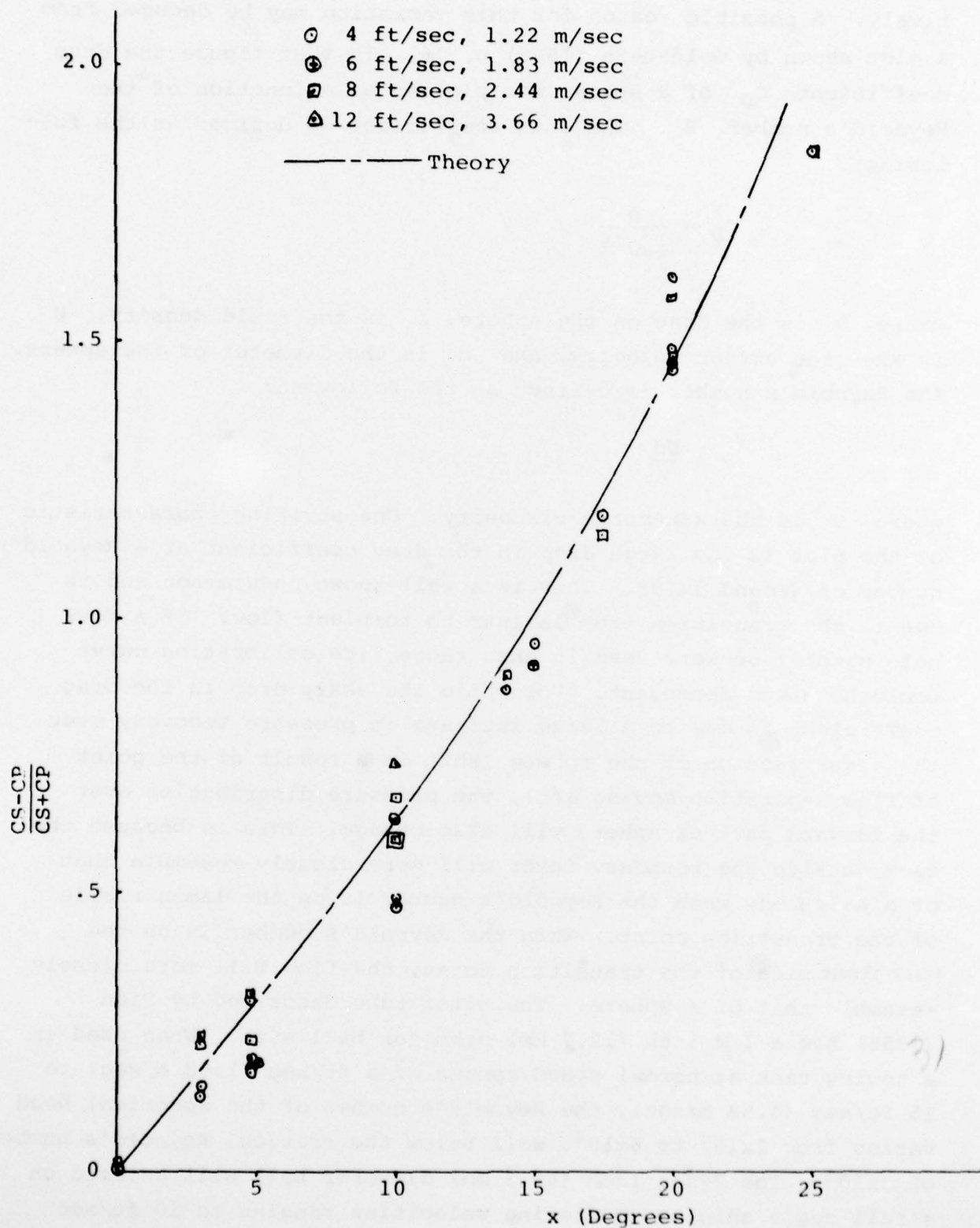


Figure 17. Five Hole Pitot Tube Calibration (without sand)



the starboard hole, and the center hole and the port hole respectively. A possible reason for this variation may be deduced from a plot shown by Goldstein (1965) p. 16. In that figure the drag coefficient  $C_D$  of a sphere was plotted as a function of the Reynold's number  $R$ . The drag coefficient is defined as the following:

$$C_D = \frac{D}{\frac{1}{2}\rho U^2 d}$$

where  $D$  is the drag on the sphere,  $\rho$  is the fluid density,  $U$  is the free stream velocity, and  $d$  is the diameter of the sphere. The Reynold's number is defined as the following:

$$R = \frac{Ud}{\nu}$$

where  $\nu$  is the kinematic viscosity. One striking characteristic of the plot is the large drop in the drag coefficient at a Reynold's number of around  $3 \times 10^5$ . This is a well-known phenomenon and is due to the transition from laminar to turbulent flow. If a five hole pitot tube were used in this range, its calibration curve would be speed dependent. For while the sharp drop in the drag coefficient is due to a large increase in pressure recovery over the *after* section of the sphere (this is a result of the point of flow separation moving aft), the pressure distribution over the forward part of sphere will also change. This is because the flow outside the boundary layer will more closely resemble that of a half-body when the Reynold's number is on the laminar side of the transition point. When the Reynold's number is on the turbulent side of the transition point, the flow will more closely resemble that of a sphere. The pitot tube described by Pien (1958) had a 1/2 inch (12.7 mm) diameter ball size. When used in a towing tank at normal speed ranges of 5 ft/sec (1.53 m/sec) to 15 ft/sec (4.58 m/sec), the Reynold's number of the spherical head varies from  $2 \times 10^4$  to  $6 \times 10^4$ , well below the critical Reynold's number of  $3 \times 10^5$ . The 2-3/8 inch (60.3 mm) diameter ball will be used on a full scale ship, encountering velocities ranging to 10 ft/sec

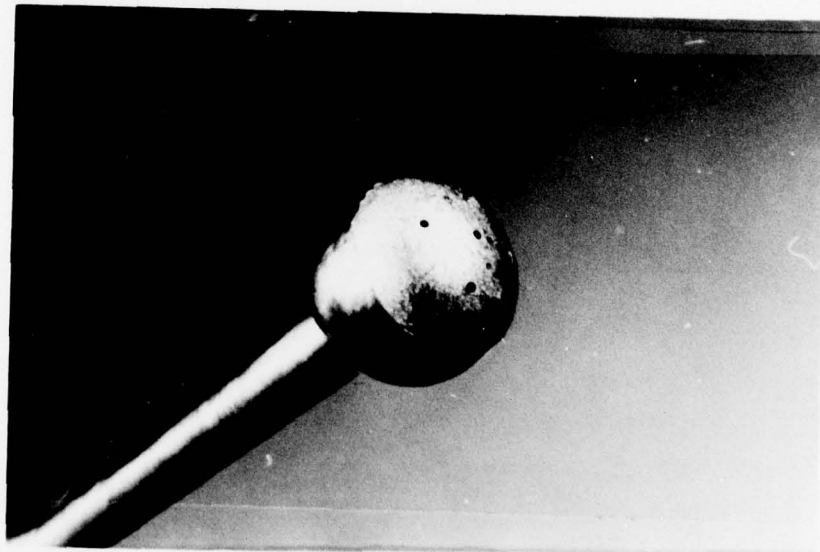


Figure 18. Five Hole Pitot Tube with Sand Added

(3.06 m/sec) to 30 ft/sec (9.18 m/sec). The Reynold's number corresponding to these flows will vary from  $2 \times 10^5$  to  $6 \times 10^5$ . Thus the full scale speed range will include speeds where there is a transition from laminar turbulent flow.

In an effort to solve the problem associated with the critical Reynold's number, fine sand granules were glued on the front of the sphere. Figure 18 shows a close up of the pitot head. To keep the less firmly attached particles from washing off, a thin coat of lacquer was applied over the sand. The pitot tube was then tested and the results are shown in Figure 19 where the non-dimensional pressure coefficient,  $(-C_S + C_P)/(C_S + C_P)$ , is plotted as a function of incident flow heading angle,  $\alpha$ . It appears that the addition of the sand has made the pressure coefficient independent of Reynold's number, at least over the speed range tested. The dashed line in the figure is a theoretical curve based on the analysis done by Pien (1958).

A measure of the level of scatter with the sand attached was obtained by estimating the carriage speed and comparing that value with the actual speed. The procedure for finding the velocity components followed the method given by Pien (1958). A set of curves were faired through the data for values of  $(C_S - C_P)/(C_S + C_P)$ ,  $C_S/V_h^2$ , etc. as a function of the incident flow angles. The actual pressure readings from the test were then used to enter the curves to estimate a heading angle and velocity components. The estimated carriage velocity based upon pitot tube measurements was then compared to the velocity from the carriage speed indicator. In Figure 20, the relative number of times a data point occurred within a given error band is plotted against the relative error. As can be seen by the figure, more than 70% of the readings had a relative error of 1% or less.

Different types of coatings over the sand granules were applied to a test piece of brass. The piece was then placed in a salt bath for two weeks to see which coating worked best. Based upon that test, a coating composed of a thinned solution of epoxy glue was selected as having adequate properties.

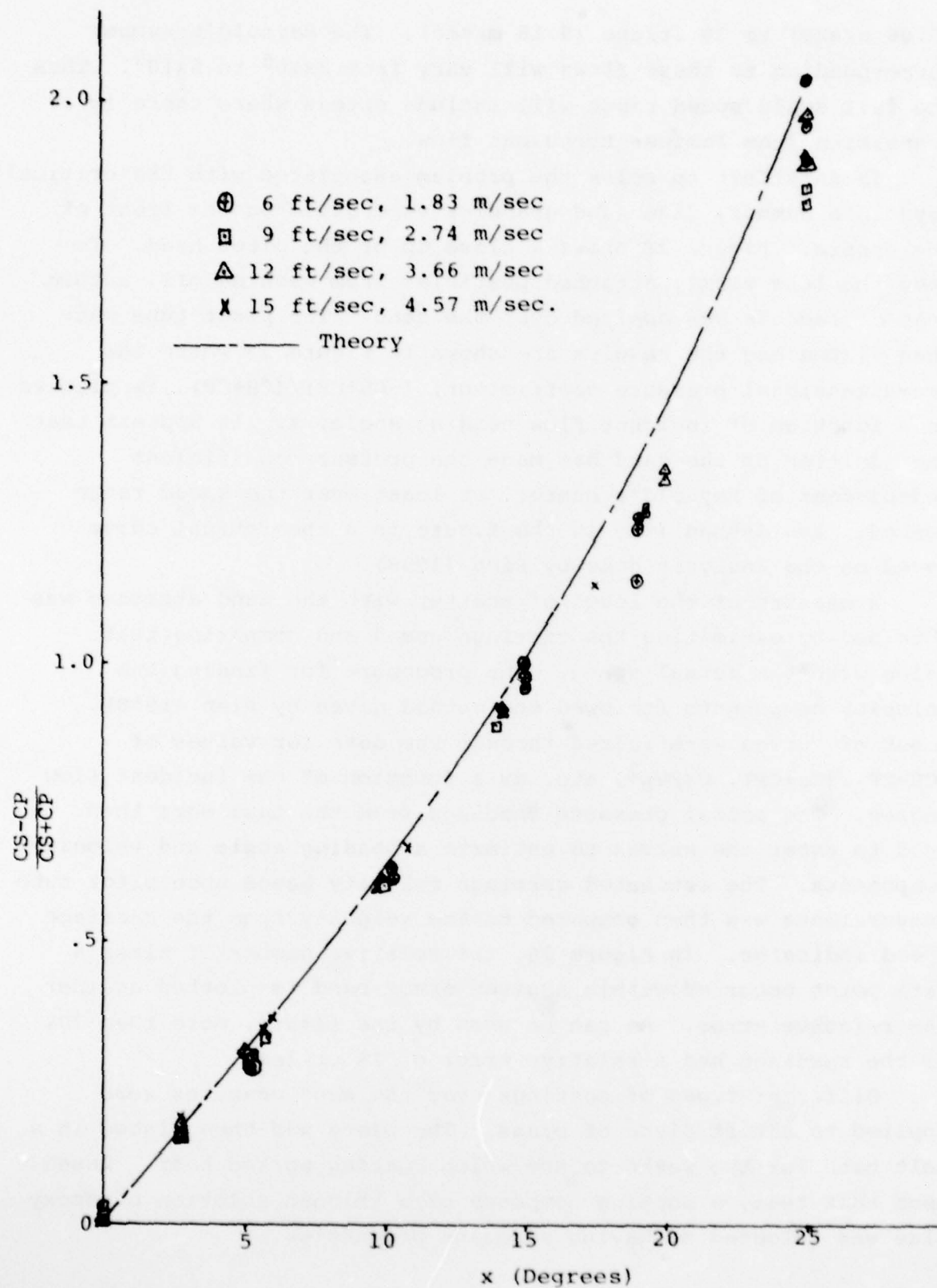


Figure 19. Five Hole Pitot Tube Calibration (with sand)



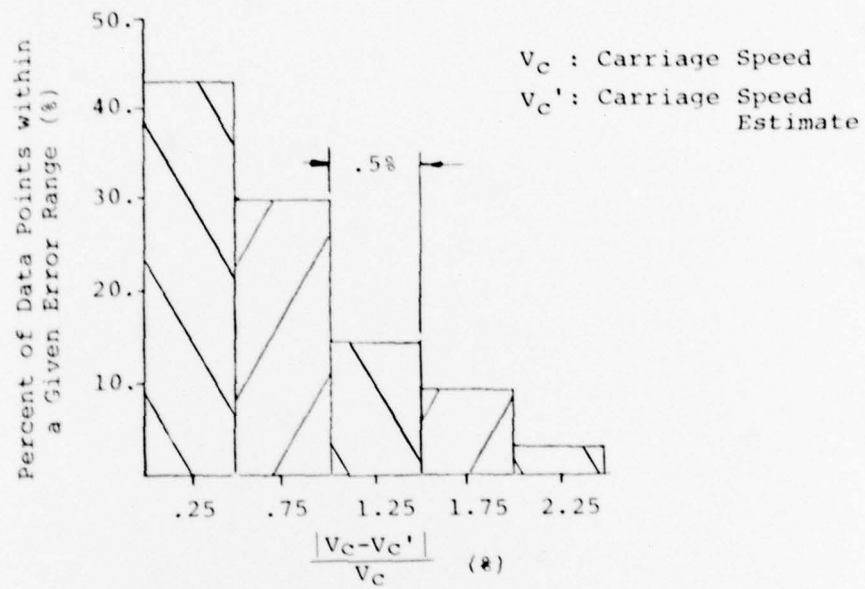


Figure 20. Relative Error in Carriage Speed Prediction  
 (Based on 69 data points)

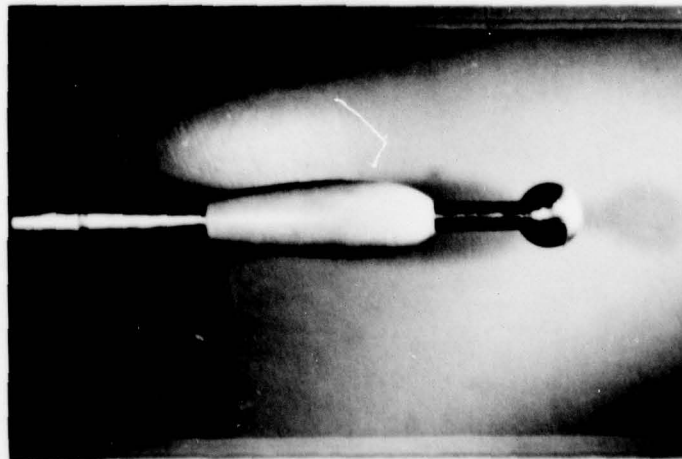


Figure 21. Five Hole Pitot Tube with Fairing Added

Even though the tank tests indicated that a reasonable level of accuracy had been attained with the addition of sand on the pitot head, a recommendation to use this type of turbulence stimulation was not made. This was due to the following considerations:

- i) The calibration curves were very sensitive to the placement of sand around the tube holes. When one particle washed off, there was a corresponding change in the  $CP/V^2$  curve. Different techniques were tried to insure a secure bonding of the particles in the vicinity of the holes; some were successful. However these proved to be very time consuming processes.
- ii) It was feared that in a salt water environment, the slime build-up on the epoxy coating would reduce the roughness of the pitot tubes, thus negating any effect the sand particles might have.
- iii) Experience in wind tunnels has indicated that the amount of turbulence in the upstream flow has a marked effect on the drag coefficient of a sphere near its transition Reynold's number. For example, see Goldstein (1965). It was felt that there would be sufficient turbulence in the wake region of a ship to make the addition of sand a redundant measure.

Takahashi, et al (1971) has suggested that a correction be made to account for the differences in head between the top hole, the center hole and the bottom hole. However, this means it would be necessary to locate the position of the air-water interface in the top tube. From visual observations, it seemed that the interface was very near to the surface of the sphere. Whether this would be true though for all speeds and all heading angles encountered we cannot say. When these differences in head were included in the calculations of the pressure coefficients, they were found to have a negligible effect for the range of speeds tested and subsequently were ignored.

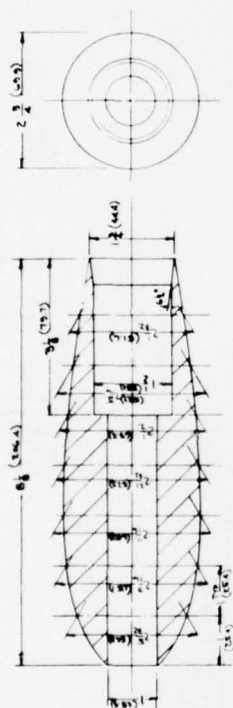
The pitot tube assembly was also tested with a fairing attached to the stem as shown in Figure 21. The purpose of this test was to determine whether the stem could be shortened. This would reduce any vibration problems associated with stem length. After a series of calibration runs, the results were compared with those from the pitot tube without the fairing and it was found that there was no significant difference. Thus the stem length could be shortened down to 3 inches (7.62 cm) without noticeably influencing the pressure distribution.

## REFERENCES

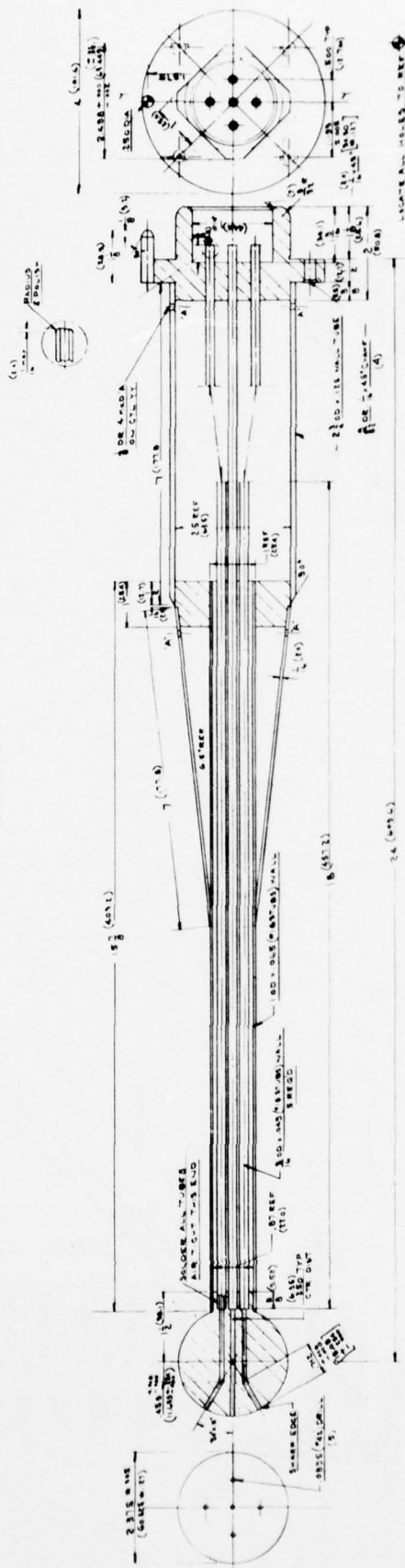
- Canham, H.J.S., "Resistance, Propulsion and Wake Tests with *HMS Penelope*," The Royal Institution of Naval Architects, Spring Meeting, 1974.
- Executive Committee for the Project of Ship Boundary Layer Measurements, "Measurement of Boundary Layer of Ships," Reports of Research Institute for Applied Mechanics, Kyushu University, Vol. XIX, No. 63, 1971.
- Goldstein, S., Modern Developments in Fluid Dynamics, Dover Publications Inc., New York, 1965.
- Namimatsu, M., et al, "Wake Distribution of Ship and Model on Full Ship Form," (Jap.), Journal of the Society of Naval Architects of Japan, Vol. 134, 1973.
- Namimatsu, M., and Muraoka, K., "The Wake Distribution of Full Form Ship," IHI Engineering Review, Vol. 7, No. 3, 1974.
- Pien, P.C., "The Five-Hole Spherical Pitot Tube," DTMB Report No. 1229, 1958.
- Takahashi, H., et al, "Measurement of Velocity Distribution Ahead the Propeller Disk of the Ship," (Jap.), Journal of the Society of Naval Architects of West Japan, Vol. 129, 1970.
- Taniguchi, K., and Fujita, T., "Comparison of Velocity Distribution in the Boundary Layer Between Ship and Model," Journal of the Society of Naval Architects of Japan, Vol. 127, 1970.
- Yokoo, K., "Measurement of Full Scale Wake Characteristics and Their Prediction from Model Results--State of the Art," Symposium on High Powered Propulsion of Large Ships, Wageningen, 1974.



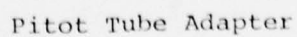




Fairing



5 Hole Pitot Tube



# INITIAL DISTRIBUTION

## Copies

2 CHONR  
 1 Code 438  
 1 Lib  
 1 USNA  
 1 Lib  
 4 NAVSEA  
 2 NAVSEA 05R  
 2 NAVSEA 05H  
 12 DDC  
 1 BUSTAND/KLEANOFF  
 1 US COAST GUARD (G-ENE-4A)  
 1 U CAL BERKELEY/DEPT NAME  
 1 CIT  
 1 Aero Lib  
 1 U IOWA  
 1 IHR/LANDWEBER  
 1 MIT  
 1 Ocean Engr/Lib  
 1 U MICHIGAN  
 1 NAME Lib  
 1 U MINNESOAT SAFHL  
 1 Killen

## Copies

1 PENN STATE U ARL  
 1 Lib  
 1 SIT DAVIDSON LAB  
 1 Lib  
 1 HYDRONAUTICS  
 1 Lib

## CENTER DISTRIBUTION

Copies	Code	
1	15	
1	152	
1	1524	
1	154	
1	156	Hagen
1	1556	Santore
1	1962	Zaloumis
1	522.1	Library (C)
1	522.2	Library (A)